

Inverse design of nonlinear phononic crystal configurations based on multi-label classification learning neural networks

Kunqi Huang(黄坤琦), Yiran Lin(林懿然), Yun Lai(赖耘), and Xiaozhou Liu(刘晓宙)

Citation: Chin. Phys. B, 2024, 33 (**10**): 104301. DOI: 10.1088/1674-1056/ad6b85
Journal homepage: http://cpb.iphy.ac.cn; http://iopscience.iop.org/cpb

What follows is a list of articles you may be interested in

Acoustic radiation force on a cylindrical composite particle with an elastic thin shell and an internal eccentric liquid column in a plane ultrasonic wave field

Rui-Qi Pan(潘瑞琪), Zhi-Wei Du(杜芷玮), Cheng-Hui Wang(王成会), Jing Hu(胡静), and Run-Yang Mo(莫润阳)
Chin. Phys. B, 2024, 33 (**9**): 094302. DOI: 10.1088/1674-1056/ad5d66

Behaviors of cavitation bubbles driven by high-intensity ultrasound

Chen-Yang Huang(黄晨阳), Fan Li(李凡), Shi-Yi Feng(冯释毅), Cheng-Hui Wang(王成会), Shi Chen(陈时), Jing Hu(胡静), Xin-Rui He(何芯蕊), and Jia-Kai Song(宋家凯)
Chin. Phys. B, 2024, 33 (**2**): 024301. DOI: 10.1088/1674-1056/ad0717

Effects of confining pressure and pore pressure on multipole borehole acoustic field in fluid-saturated porous media

Zhi-Qiang Zhao(赵志强), Jin-Xia Liu(刘金霞), Jian-Yu Liu(刘建宇), and Zhi-Wen Cui(崔志文)
Chin. Phys. B, 2024, 33 (**1**): 014301. DOI: 10.1088/1674-1056/acf9e6

Dynamics of magnetic microbubble transport in blood vessels

Jie Chen(陈杰), Chenghui Wang(王成会), and Runyang Mo(莫润阳)
Chin. Phys. B, 2023, 32 (**9**): 094302. DOI: 10.1088/1674-1056/aca14b

Nonlinear wave propagation in acoustic metamaterials with bilinear nonlinearity

Shiqi Liang(梁诗琪), Jiehui Liu(刘杰惠), Yun Lai(赖耘), and Xiaozhou Liu(刘晓宙)
Chin. Phys. B, 2023, 32 (**4**): 044301. DOI: 10.1088/1674-1056/ac9783

Inverse design of nonlinear phononic crystal configurations based on multi-label classification learning neural networks

Kunqi Huang(黄坤琦)[1,2], Yiran Lin(林懿然)[1,2], Yun Lai(赖耘)[1,2,†], and Xiaozhou Liu(刘晓宙)[1,2,3,‡]

[1] *Key Laboratory of Modern Acoustics, Institute of Acoustics, Nanjing University, Nanjing* 210093, *China*
[2] *School of Physics, Collaborative Innovation Center of Advanced Microstructures, Nanjing University, Nanjing* 210093, *China*
[3] *State Key Laboratory of Acoustics, Institute of Acoustics, Chinese Academy of Sciences, Beijing* 100190, *China*

(Received 22 June 2024; revised manuscript received 31 July 2024; accepted manuscript online 6 August 2024)

Phononic crystals, as artificial composite materials, have sparked significant interest due to their novel characteristics that emerge upon the introduction of nonlinearity. Among these properties, second-harmonic features exhibit potential applications in acoustic frequency conversion, non-reciprocal wave propagation, and non-destructive testing. Precisely manipulating the harmonic band structure presents a major challenge in the design of nonlinear phononic crystals. Traditional design approaches based on parameter adjustments to meet specific application requirements are inefficient and often yield suboptimal performance. Therefore, this paper develops a design methodology using Softmax logistic regression and multi-label classification learning to inversely design the material distribution of nonlinear phononic crystals by exploiting information from harmonic transmission spectra. The results demonstrate that the neural network-based inverse design method can effectively tailor nonlinear phononic crystals with desired functionalities. This work establishes a mapping relationship between the band structure and the material distribution within phononic crystals, providing valuable insights into the inverse design of metamaterials.

Keywords: multi-label classification learning, nonlinear phononic crystals, inverse design

PACS: 43.25.+y **DOI:** 10.1088/1674-1056/ad6b85

1. Introduction

When mechanical waves propagate in phononic crystals, they tend to exhibit unique bandgap properties due to wave scattering or local resonance in the structure.[1] In recent years, the incorporation of nonlinearity into phononic crystal systems has significantly expanded the realm of wave propagation not achievable in linear systems. For instance, nonlinear systems can display novel wave phenomena such as soliton propagation, higher-order harmonic generation, and nonreciprocal wave transmission, which hold considerable practical significance.[2–5] In nonlinear phononic crystals, as mechanical waves travel through the material, energy can be converted into waves at higher frequencies. This is a process known as second-harmonic generation. Second harmonic generation is a common occurrence in nonlinear crystals, but designing an ideal nonlinear phononic crystal remains a challenging task due to the inherent non-uniformity of the material and the complexity in calculations.[5–7]

Over the past few decades, researchers have designed phononic crystals by tuning the physical parameters of the materials to match specific dispersion characteristics.[8,9] This traditional method requires empirical and experimental support, and the design process is complex, consuming a lot of time and computer memory. In recent years, artificial intelligence technology has developed rapidly. Neural networks, as a crucial component of artificial intelligence technology, have found widespread application across various fields including computer vision, speech recognition, and natural language processing. Inspired by advances in artificial intelligence technology, the use of neural networks in the design of metamaterials has increasingly garnered attention.[10–14] For example, Peurifoy *et al*. trained a neural network to approximate the light scattering properties of multilayered nanospheres.[15] Finol *et al*. used a deep convolutional neural network and a conventional densely connected neural network to predict the eigenvalues of phononic crystals and concluded that the convolutional neural network outperformed the conventional densely connected neural network.[16] Kollmann *et al*. applied the ResUNet convolutional neural network model for the optimization design of metamaterials.[17] Li *et al*. employed an autoencoder and multilayer perceptron models to establish an intrinsic connection between the two-dimensional phononic crystal image features, structural topology features, and bandgap characteristics.[18] Gurbuz *et al*. proposed a method based on generative adversarial neural networks to design acoustic metamaterials, successfully implementing inverse design of unit cells.[19] Wei *et al*. proposed a general method based on the gradient descent method to study the inverse design of one-dimensional (1D) phononic crystals.[20] The variational autoencoder model have been used

†Corresponding author. E-mail: laiyun@nju.edu.cn
‡Corresponding author. E-mail: xzliu@nju.edu.cn

© 2024 Chinese Physical Society and IOP Publishing Ltd

to study the inverse design problem by Ahmed *et al*. and Du *et al*.[21,22] Ahmed *et al*. focused on the design of a broadband acoustic cloak, while Du *et al*. explored the design of a grating structure based acoustic wavelength division multiplexing device.[21,22] Huang *et al*. adopted both convolutional neural networks and general regression neural networks in the design of nonlinear phononic crystals.[23]

The foregoing research illustrates the viability of utilizing neural network methodologies for the inverse design of phononic crystal structures. However, current researches mainly focus on predicting the fundamental parameters of target linear phononic crystals. Due to the complexity of nonlinear phononic crystal calculations, its design using neural networks is more challenging. Additionally, a practical issue arises where predicted material parameters might not correspond to readily available materials in reality. To tackle this challenge, we opt to utilize existing materials as constituents for the construction of phononic crystals. We assume each layer of a multilayer structured nonlinear phononic crystal is composed of a realistic material. This approach yields a diverse sample of phononic crystal structures. Subsequently, because nonlinear phononic crystals have more complex responses and it is difficult to obtain analytical solutions for the spectrum response curves, we have calculated the transmission curves of all the samples using the ode45 Longo Kuta method in order to obtain their energy band structure distributions. Then, the mapping relationship between the band structure and the phononic crystal structure is established by the neural network. Finally, after evaluating the prediction performance of the neural network, we have successfully established the mapping relationship between the band structure and the material distribution of phononic crystals based on Softmax logical regression (SLR) and multi-label classification learning (MLCL) method, and realized the inverse design of nonlinear phononic crystals.

2. Theoretical analysis

2.1. Nonlinear phononic crystal models

It is well known that the energy band structure of phononic crystals is dependent on the composition and arrangement of different materials. Here, we simulate wave propagation in 1D layered nonlinear phononic crystals made of a variety of different materials and different arrangements. Then the wave propagation data are used to provide a large amount of training data for neural network construction.

The model generating the dataset is depicted in Fig. 1. Consider longitudinal wave propagation in the one-dimensional nonlinear phononic crystal. The structure consists of alternating N-layer linear elastic materials with different material combinations, which produce phononic crystals with different topological configurations corresponding to different energy band structures. Each layer of the phononic crystal has the same thickness and the j-th layer is filled with one of m different materials, identified by the number between 1 and m according to the material filled. They are embedded between two linearly elastic semi-infinite media with the same properties as material 1. All these linear elastic materials can be regarded as interconnected at the interface through $N+1$ nonlinear elastic interfaces. With different layered materials, the configurations can be represented by a 1D array, where ρ_j and c_j denote the density and sound velocity of the j-th layer, respectively.

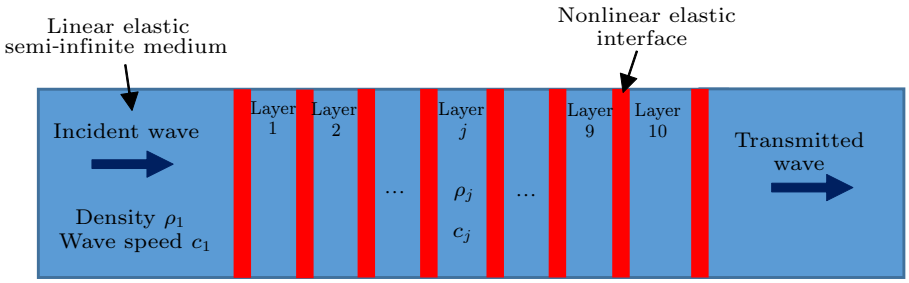


Fig. 1. One-dimensional nonlinear phononic crystal model with nonlinear interfaces.

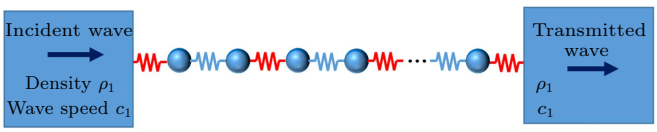


Fig. 2. Discretized model of the nonlinear phononic crystal (finite waveguide is approximated as a linearly coupled oscillator, and the interface interaction is nonlinear coupling).

The wave propagation phenomena in this nonlinear system are difficult to solve accurately in analytical form, so a discrete mass-spring model of the structure (as shown in Fig. 2) is developed here for analysis. This is a classical approach that can be easily implemented for the numerical analysis of this nonlinear structure.[24–29]

Although the masses in the figure are of the same color, here we consider that they belong to different materials. The equations of motion of this structure are analyzed as follows.

With an initial incentive

$$u_{\text{inc}}(x-c_1t)=A\cos\left(\omega c_1^{-1}(x-c_1t)\right), \tag{1}$$

where u is the mass displacement, A is the initial amplitude, ω is the angular frequency of the wave, and t is the time. If the n-th layer is a linear elastic layer i ($i=1$ or 2), its corresponding equation of motion is

$$\frac{\rho_i h_i}{2}\ddot{u}_{n,1}+\frac{2\rho_i c_i^2}{h_i}\left(u_{n,1}-u_{n,2}\right)=-f\left(u_{n,1}-u_{n-1,2}\right), \tag{2}$$

$$\frac{\rho_i h_i}{2}\ddot{u}_{n,1}-\frac{2\rho_i c_i^2}{h_i}\left(u_{n,1}-u_{n,2}\right)=f\left(u_{n+1,1}-u_{n,2}\right), \tag{3}$$

where $u_{n,1}$ and $u_{n,2}$ denote the displacements of the first and second masses of the n-th layer. f denotes the nonlinear interface interaction force.

In the case of the spring-type interface with weak quadratic nonlinearity, the nonlinear interface equation is

$$f(\Delta u)=K(1-\beta\Delta u)\Delta u. \tag{4}$$

In Eq. (4), K is the linear interface stiffness, β is a positive parameter representing the nonlinearity of the interface, and Δu represents the relative displacement at the interface.

The boundary conditions of the model are

$$\begin{aligned}\rho_1c_1\dot{u}_0 &= K(u_{1,1}-u_0)-\beta K^2(u_{1,1}-u_0)^2\\ &\quad -2\rho_1c_1^2u_{\text{inc}}(-c_1t),\end{aligned} \tag{5}$$

$$\rho_1c_1\dot{u}_{N+1}=-K(u_{N+1}-u_{N,2})+\beta K^2(u_{N+1}-u_{N,2})^2, \tag{6}$$

where u_0 is the end of the first semi-infinite medium, which is the displacement at $x=0$, and u_{N+1} is the beginning of the second semi-infinite medium.

Rearranging the above equation gives

$$\begin{aligned}\dot{u}_0 &= \frac{K}{\rho_1c_1}(u_{1,1}-u_0)-\frac{\beta K^2}{\rho_1c_1}(u_{1,1}-u_0)^2\\ &\quad -2A\omega\sin(\omega t),\end{aligned} \tag{7}$$

$$\begin{aligned}\ddot{u}_{n,1} &= -\frac{4c_i^2}{h_i^2}\left(u_{n,1}-u_{n,2}\right)-\frac{2K}{\rho_ih_i}\left(u_{n,1}-u_{n-1,2}\right)\\ &\quad +\frac{2\beta K^2}{\rho_ih_i}\left(u_{n,1}-u_{n-1,2}\right)^2,\end{aligned} \tag{8}$$

$$\begin{aligned}\ddot{u}_{n,2} &= \frac{4c_i^2}{h_i^2}\left(u_{n,1}-u_{n,2}\right)+\frac{2K}{\rho_ih_i}\left(u_{n+1,1}-u_{n,2}\right)\\ &\quad -\frac{2\beta K^2}{\rho_ih_i}\left(u_{n+1,1}-u_{n,2}\right)^2,\end{aligned} \tag{9}$$

$$\dot{u}_{N+1}=-\frac{K}{\rho_1c_1}\left(u_{N+1}-u_{N,2}\right)+\frac{\beta K^2}{\rho_1c_1}\left(u_{N+1}-u_{N,2}\right)^2. \tag{10}$$

We can use Eqs. (7)–(10) to solve the numerical solution for the displacements at the end of this structure in the ODE45 solver. After obtaining the displacement signal at the end of the waveguide, the second harmonic amplitude $A_{2\omega}$ is obtained by processing the steady state signal using the fast Fourier transform. In order to better extract the features, the transmission spectral profile of the second harmonic can be obtained by calculating the transmittance based on

$$T=10\log\left|\frac{A_{2\omega}}{\beta A^2}\right|. \tag{11}$$

2.2. Getting the dataset

In order to obtain the dataset that can be used for MLCL neural networks, for this model, the choice of the material for each layer is the main variable that affects the second harmonic behavior. The material selection problem involves the classification function of the neural network. Therefore, the input of this neural network should be the band structure of the second harmonic transmission curve and the output is N parallel layers, each of which outputs the corresponding material parameters.

The layers of nonlinear phononic crystals should not be chosen too few, which tends to lead to a lack of diversity in the band structure of the training samples. It is also not advisable to have too many layers, which may make the training more difficult. Therefore we choose the number of phonon crystal layers N as 10. In order to make the first passband and stopband of the transmission curves fall in the range of 0 to 1 MHz as much as possible, we chose the materials in Table 1 to form the nonlinear phonon crystal layer. The materials selected are aluminum, steel, and magnesium, and the common parameters of the constituent materials are shown in Table 1. The other parameter settings are: each layer's thickness h is 0.003 m, linear stiffness K is 6×10^{13} N/m, nonlinear coefficient β is 5×10^3, and initial excitation amplitude A is 5 μm. We number three materials as 1, 2, and 3 and randomly fill them in 10 layers, then 3^{10} phononic crystal configurations are obtained. So each phonon crystal configuration can then be represented by a 10-bit array of 1, 2, and 3 randomly arranged.

Table 1. Material parameters of aluminum, steel, and magnesium.

Material	Serial number	Densities (kg/m^3)	Sound velocity (m/s)
Aluminum	1	2680	6420
Steel	2	7860	6073
Magnesium	3	1800	6055

In these nonlinear phononic crystal configurations, because of the translational symmetry, it may happen that phononic crystals of different configurations correspond to the same distribution of band structures. Translation symmetry means that one array will be equal to another after translation. For example, the arrays 1112233111 and 1111112233 exhibit translational symmetry, and arrays of this type will correspond to the same band structure. This data with different configurations corresponding to the same band structure will interfere with the neural network training and thus reduce the generalization of the neural network. Therefore, we need to filter the

phononic crystal configurations with translational symmetry and keep only one configuration to optimize the neural network training. In addition to this, we need to exclude configurations in which the band gap does not exist to avoid increasing the learning difficulty of the neural network.

From the filtered phononic crystal configurations, we selected 3000 sets as datasets for the neural network, including 2700 sets as the training set and 300 sets as the testing set. After obtaining the second harmonic transmission curves of nonlinear phononic crystals, further features need to be extracted to be used as training data available for neural networks. The detailed steps are as follows: determining the frequency range of the passband and stopband of the second harmonic according to the transmission curve. Then the entire frequency range is divided into multiple small intervals, and the thresholds are set to determine whether each small interval belongs to the passband or stopband. We use the number 1 to denote the passband and the number 0 to denote the stopband. So that the band structure of the second harmonic can be represented by a simple 1D array of 1 and 0.

In this paper we use the MLCL neural network to construct a mapping between second harmonic band features and material-type composition.

3. Principle and basic structure of multi-label classification neural network

MLCL neural network is a neural network model for dealing with multi-label classification problems. In the multi-label classification problem, each sample can be assigned to many categories, unlike the traditional single-label classification problem, in which each sample can belong to only one category. Multi-label classification problems are common in real-life situations, such as image recognition where a picture may contain multiple objects, each of which needs to be correctly labeled. This also has applications in natural language processing, such as in topic categorization of news articles, where a single article may cover more than one topic. In this paper, the MLCL neural network is used to classify the material components of nonlinear phononic crystal multilayer structures, which solves the problems of finding effective materials in reality and having simple material distribution in previous research methods. We mainly use Softmax logistic regression and MLCL neural networks. Softmax logistic regression is used to implement the selection of material type classification of the layered structure. MLCL, i.e., having multiple outputs and being able to process multiple tasks simultaneously, is used to determine the distribution of materials in each region. The model of the neural network is shown in Fig. 3.

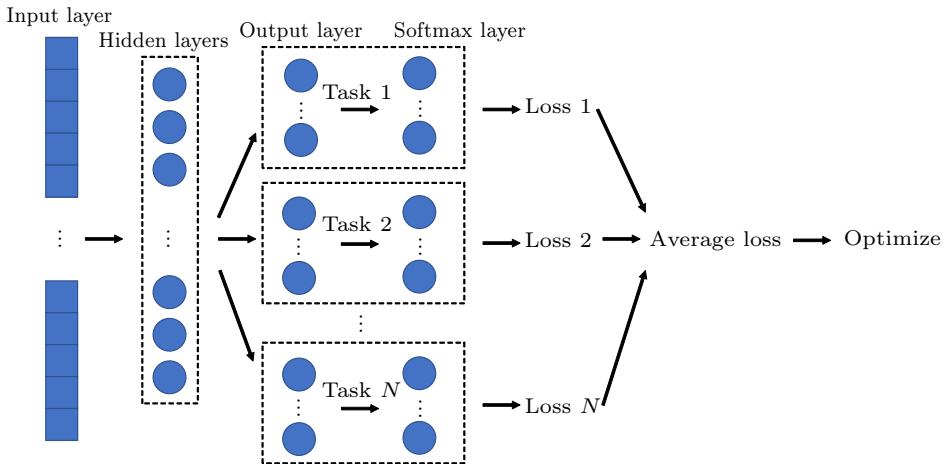


Fig. 3. The MLCL neural network model diagram.

The MLCL neural network, consists of an input layer, a hidden layer, an output layer, and a Softmax layer, where the neurons of the neighboring layers are connected to form the overall neural network model. The input data of each sample enter the input layer through forward propagation. Subsequently, each layer of the network performs numerical calculations using the output data of the previous layer as the input data and passes the results of the calculations to the next layer. This process of information transfer and computation in each layer constitutes the forward propagation of the neural network.

When data pass through the hidden layer of the neural network, the exact computational process involves two main steps: weighting and activation. The weighting process is when the data pass through the hidden layer it will multiply all the neuron outputs of the previous layer with the weight coefficients matrix and accumulate them and add the accumulated result with the bias parameter of this layer to get the inputs of the neurons. The activation process is a nonlinear transformation of the weighted inputs through an activation function to

introduce nonlinearity in the network.

After the computation in the hidden layer, the data were imported into N parallel output layers. Each output layer is responsible for outputting the parameter values of the material of the corresponding layer to describe the phononic crystal configuration. Unlike the hidden layer, the output layer does not require an activation function, but rather by linearly transforming the output of the previous layer and passing the result to the final Softmax layer. This is designed to directly output the raw values of each output layer, while the Softmax layer is used to normalize these values into probability distributions for efficient multi-category classification. This structure allows the neural network the flexibility to handle multiple parallel tasks. The computational process of the Softmax layer is designed to convert the network output into a probability distribution. In particular, the Softmax function converts the original output value of a vector into a set of probability values such that the sum of these probability values is equal to 1. Given a vector $z = [z_1, z_2, \ldots, z_m]$, the Softmax function is computed as follows:

$$\mathrm{Softmax}(z)_i = \frac{\mathrm{e}^{z_i}}{\sum_{j=1}^{m} \mathrm{e}^{z_j}}, \tag{12}$$

where $\mathrm{Softmax}(z)_i$ denotes the i-th element of the Softmax function's output, and e is the base of the natural logarithm. the output of the Softmax layer is a probability distribution, with each element denoting the probability of the corresponding category. Typically, the neural network selects the categories as those with the highest probability.

Then we measure the difference between the model output and the actual label by means of the cross-entropy function which is used as a loss function. For the multicategorization problem, assuming that the model has m output categories, the actual labels are t, and the output of the model is y (denoting the predicted probability of each category), the multicategorization cross-entropy loss function L is formulated as

$$L(y,t) = -\sum_{i=1}^{m} t_i \log(y_i), \tag{13}$$

where t_i is the ith element of the actual label and y_i is the i-th element of the model's predicted output. This formula weights and takes the negative sign of the predicted probabilities for all categories to get the final loss value. In practical training, the smaller the cross-entropy loss, the closer the model output is to the actual label. Therefore the goal of the optimization algorithm is usually to minimize the cross-entropy loss. Because there are N labels in the nonlinear phononic crystal inverse design in this paper, we need to average the cross-entropy loss of N tasks as the total loss function. Finally, it is optimized by back propagation algorithm to achieve the suitable accuracy requirement.[30]

In addition, we need to define the correctness of the predictions for the training and testing sets. Predictive correctness of training set and testing set is a metric used to evaluate performance during the training. The prediction correctness Trainacc and Testacc of the training and testing sets are defined in the following equation:

$$\begin{aligned} \mathrm{Train_{acc}}, \mathrm{Test_{acc}} &= \frac{1}{M_{\mathrm{Train}}, M_{\mathrm{Test}}} \frac{1}{m} \\ &\quad \times \sum_{a=1}^{M_{\mathrm{Train}} M_{\mathrm{Teat}}} \sum_{b=1}^{m} [\mathrm{Eq}(\hat{y}_{ab}, y_{ab})], \\ \mathrm{Eq}(\hat{y}_{ab}, y_{ab}) &= 1,\ \hat{y}_{ab} = y_{ab}, \\ \mathrm{Eq}(\hat{y}_{ab}, y_{ab}) &= 0,\ \hat{y}_{ab} \neq y_{ab}, \end{aligned} \tag{14}$$

where M_{Train} and M_{Test} denote the numbers of samples in the training and testing sets, and $\hat{y}_{ab}$ and y_{ab} denotes the predicted and true values of the b-th label of the a-th sample. Too many neurons may lead to overfitting, while too few neurons may lead to underfitting. Therefore, the method of verifying the performance of the testing set is used to determine the appropriate number of neurons. When the correctness of the predictions are as expected, it indicates that the neural network can successfully construct the mapping relationship between the harmonic band structure and the material arrangement.

4. Results and discussion

The inverse design process is shown in Fig. 4. First, we set the frequency range under study to 0 MHz–1 MHz so that the first passband and first stopband of each sample are included in the studied frequency range as much as possible. Then we use 1000 Hz as the unit frequency to divide the whole frequency range and set the threshold to determine the unit frequency is whether passband or stopband. This threshold is determined by both the transmission curve shape and the design goals. Based on the shape of the existing transmission curve, the threshold is set to -80 dB. The passband is set to 1 and the stopband is set to 0 according to the threshold. The band features of the target transmission curve are represented by a 1D 0–1 array, which is then fed to the trained neural network. The network outputs the desired material distribution for each layer, from which the predicted second harmonic transmission curve can be obtained.

We study the inverse design of a 1D nonlinear phononic crystal composed of three materials: aluminum, steel, and magnesium. The number of hidden layers is set to have four layers, and the number of neurons in each layer is 2000, 1000, 500, and 500, respectively. To improve the overfitting phenomenon of the training process, the dropout operation is added between each hidden layer and 10% of the neurons between each layer are randomly discarded.[31] To speed up the training and overcome the gradient vanishing, the RELU function is used as the hidden layer activation function.[32] Adam's

algorithm is used to update the network parameters and optimize the total loss loss.[33]

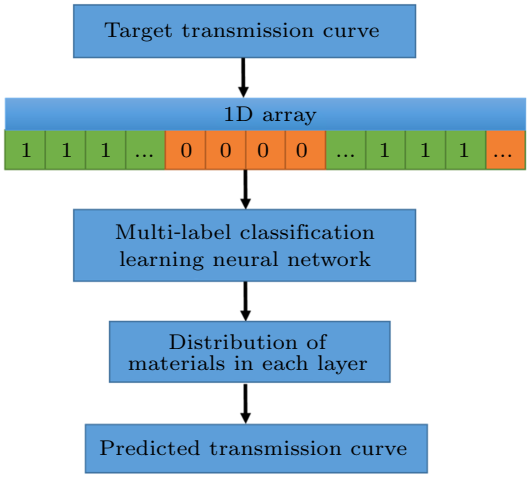


Fig. 4. Flowchart of the MLCL neural network for designing nonlinear phononic crystals.

The total loss during training (loss) and training set prediction correctness with the training i iterations (E_{poch}) are shown in Fig. 5. After 2000 iterations, the total training loss decreases from 1.05 to 0.6. The training set prediction correctness gradually increases with the number of iterations and finally stabilizes at 95%. The trained neural network is tested using testing set and its testing set predictions can be correct up to 90%.

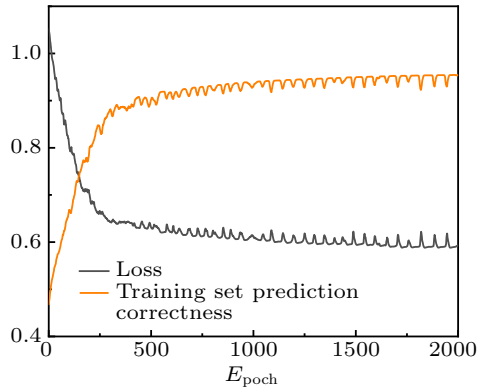


Fig. 5. Graph of loss and training set prediction correctness with iterations.

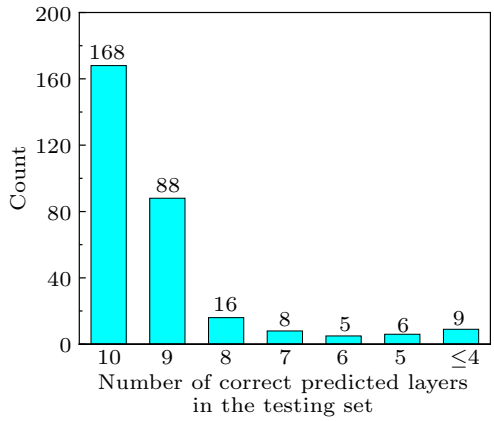


Fig. 6. The distribution of the number of correctly predicted layers in the testing set.

We need to predict the material distribution of 10 layers of phononic crystals, so we can use the number 10 to indicate that it is completely predicted correctly, with the number 9 to indicate that 9 layers are predicted correctly, and so on. As shown in Fig. 6, the distribution of the number of correctly predicted layers in the testing set, the vast majority of the dataset predicts the correct number of layers up to 8 or more, which accounts for about 80% of the total number of samples.

A sample of 9, 8, and 7 correctly predicted layers in the test set are given, respectively, and their target transmission curves and the transmission curves predicted by the neural network are made as Figs. 7–9. In the figure, the gray area is the area where the input target transmission curve is "1", and the white area is the area where the input target transmission curve is "0". ODE denotes the target transmission curve, and MLCL denotes the transmission curve computed by the MLCL neural network prediction.

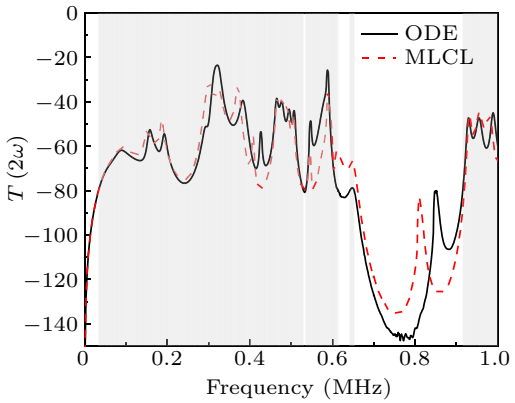


Fig. 7. Predicting the correct sample of 9 layers (ODE indicates the target transmission curve, MLCL indicates the transmission curve predicted by the MLCL neural network prediction).

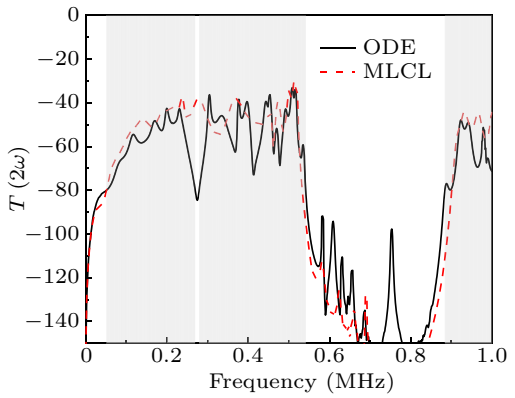


Fig. 8. Predicting the correct sample of 8 layers.

It can be seen that the samples with 8 or more correct layers of prediction have good prediction accuracy, then the samples with 8 or more correct layers of prediction can be considered as successful prediction. And the prediction correctness of the model is about 80% indicating that the prediction is satisfactory. The results demonstrate that it is possible to realize the inverse design of the material arrangement

of nonlinear phononic crystal structures based on neural networks with MLCL. Besides, since the probabilistic property of variational autoencoder helps the model to learn the statistical properties of the data distribution, variational autoencoder can be subsequently combined with existing MLCL method, which may further improve the efficiency and the accuracy of the inverse design.

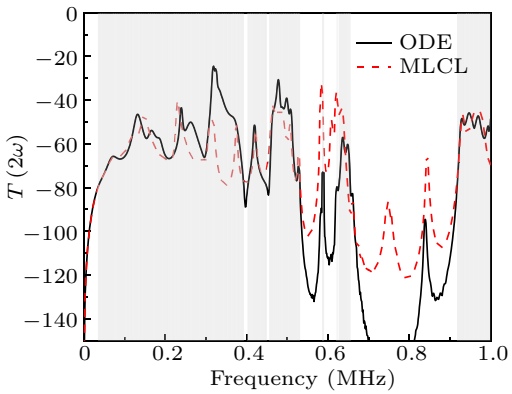


Fig. 9. Predicting the correct sample of 7 layers.

5. Conclusion

The paper transforms the phononic crystal inverse design problem into a multi-classification problem for each component material of the configuration based on MLCL neural networks. Taking the target energy band structure transmission curve as the input to the neural network, the network will directly output the material arrangement configuration of the corresponding phononic crystal. We consider the diversity and complexity of material properties and structural configurations when constructing the dataset, aiming to ensure that the neural network model is capable of effective inverse design and exhibits good generalization performance. The design method is based on real material permutations, which is easier to realize than previous methods. At the same time, the method is more efficient than traditional methods based on analytical theory and parametric analysis. Therefore, our work opens a different approach of applying the method of neural networks to solve the inverse design problem of nonlinear phononic crystals.

Acknowledgements

Project supported by the National Key Research and Development Program of China (Grant No. 2020YFA0211400), the State Key Program of the National Natural Science of China (Grant No. 11834008), the National Natural Science Foundation of China (Grant Nos. 12174192, 12174188, and 11974176), the State Key Laboratory of Acoustics, Chinese Academy of Sciences (Grant No. SKLA202410), and the Fund from the Key Laboratory of Underwater Acoustic Environment, Chinese Academy of Sciences (Grant No. SSHJ-KFKT-1701).

References

[1] Ma T, Su X, Dong H, Wang Y and Zhang C 2017 *Chin. J. Theor. Appl. Mech.* **49** 743
[2] Cabaret J, Tournat V and Béquin P 2012 *Phys. Rev. E* **86** 041305
[3] Delph T, Herrmann G and Kaul R 1979 *J. Appl. Mech.* **46** 113
[4] Biwa S, Nakajima S and Ohno N 2004 *J. Appl. Mech.* **71** 508
[5] Li Z N, Wang Y Z and Wang Y S 2021 *Proc. Royal Soc. A* **477** 20200357
[6] Ishii Y and Biwa S 2012 *AIP Conf. Proc.* **1474** 223
[7] Ishii Y and Adachi T 2019 *Dynamics and Control of Advanced Structures and Machines* pp. 65–73
[8] Wang Y F, Wang Y Z, Wu B, Chen W and Wang Y S 2020 *Appl. Mech. Rev.* **72** 040801
[9] Liu J, Guo H and Wang T 2020 *Crystals* **10** 305
[10] Liu C X and Yu G L 2023 *Journal of Computational Design and Engineering* **10** 602
[11] Jin Y, He L, Wen Z, Mortazavi B, Guo H, Torrent D, Djafari-Rouhani B, Rabczuk T, Zhuang X and Li Y 2022 *Nanophotonics* **11** 439
[12] Li Y, Chen D, Li X and Wang W 2024 *Journal of Vibration and Control* **30** 807
[13] He L, Li Y, Torrent D, Zhuang X, Rabczuk T and Jin Y 2023 *Microstructures* **3** 2023037
[14] Cui J, Li Y, Zhao C and Zheng W 2023 *Chin. Phys. B* **32** 096101
[15] Peurifoy J, Shen Y, Jing L, Yang Y, Cano-Renteria F, DeLacy B G, Joannopoulos J D, Tegmark M and Soljačić M 2018 *Sci. Adv.* **4** eaar4206
[16] Finol D, Lu Y, Mahadevan V and Srivastava A 2019 *International Journal for Numerical Methods in Engineering* **118** 258
[17] Kollmann H T, Abueidda D W, Koric S, Guleryuz E and Sobh N A 2020 *Mater. Design* **196** 109098
[18] Li X, Ning S, Liu Z, Yan Z, Luo C and Zhuang Z 2020 *Computer Methods in Applied Mechanics and Engineering* **361** 112737
[19] Gurbuz C, Kronowetter F, Dietz C, Eser M, Schmid J and Marburg S 2021 *J. Acoust. Soc. USA* **149** 1162
[20] Wei Y and He D 2023 *Chin. Phys. Lett.* **40** 090502
[21] Ahmed W W, Farhat M, Zhang X and Wu Y 2021 *Phys. Rev. Res.* **3** 013142
[22] Du Z and Mei J 2022 *Phys. Rev. Res.* **4** 033165
[23] Huang K, Li Y, Lai Y and Liu X 2023 *IEEE Open Journal of Ultrasonics, Ferroelectrics, and Frequency Control* **3** 166
[24] Zhao C, Zhang K, Zhao P and Deng Z 2022 *Nonlinear Dyn.* **108** 743
[25] Grinberg I and Matlack K 2020 *Wave Motion* **93** 102466
[26] Liang S, Liu J, Lai Y and Liu X 2023 *Chin. Phys. B* **32** 044301
[27] Chen Z, Zhou W and Lim C 2020 *International Journal of Nonlinear Mechanics* **125** 103535
[28] Wang Y Z and Wang Y S 2018 *Wave Motion* **78** 1
[29] Manimala J M and Sun C 2016 *J. Acoust. Soc. USA* **139** 3365
[30] Che Z G, Chiang T A and Che Z H 2011 *International Journal of Innovative Computing, Information and Control* **7** 5839
[31] Srivastava N, Hinton G, Krizhevsky A, Sutskever I and Salakhutdinov R 2014 *The Journal of Machine Learning Research* **15** 1929
[32] Boob D, Dey S S and Lan G 2022 *Discrete Optimization* **44** 100620
[33] Kingma D P and Ba J 2014 arXiv preprint arXiv: 1412.6980